Spin density in $MnNi_{3.55}$: A magnetic state of fcc manganese

C. Petrillo
Istituto di Struttura della Materia del Consiglio Nazionale delle Ricerche, Via Enrico Fermi 38, 00044 Frascati, Italy

F. Sacchetti
Dipartimento di Fisica dell'Università di Perugia, Perugia, Italy and Istituto di Struttura della Materia del Consiglio Nazionale delle Ricerche, Via Enrico Fermi 38, 00044 Frascati, Italy

M. Scafi
Dipartimento di Fisica dell'Università di Roma "La Sapienza," Roma, Italy
(Received 1 April 1991; revised manuscript received 28 May 1991)

The magnetic structure factors determined using polarized-neutron scattering have been employed to analyze the magnetic-moment distribution of Mn in MnX_3 alloys (X=Ni,Pt). In particular, a spin-density measurement in $MnNi_{3.55}$ at a low degree of long-range order has been performed at room temperature. Results suggest that Mn is found in a high-magnetic-moment state in this class of compounds, independently of the system, thus indicating a small dependence of the magnetic state on the atomic volume. Furthermore, a rather direct evidence of the presence of Mn atoms having a negative magnetic moment is also obtained. The information, which can be derived on the electron distribution in fcc Mn, is also discussed in a phenomenological fashion.

I. INTRODUCTION

In recent years the experimental study of charge and spin densities in transition metals embedded in different environment (alloys and compounds) has shown systematic failures[1,2] of the local-spin-density approximation[3] (LSDA) as applied to the calculation of ground state in crystals. In particular, it has been found that calculated charge and spin densities are correctly reproduced as far as the spherical part is concerned, so that rather good estimates of the magnetic moments are obtained, whereas the asphericity of the electron distribution is found only qualitatively in agreement with the experimental data.[1,2,4] Such a behavior is thought to be related to the intrinsic symmetry of Fermi and Coulomb holes as described by the LSDA.

Another systematic failure of the LSDA, still to be related to the size of Fermi and Coulomb holes, shows up in the calculation of the cohesive energy along the $3d$ transition series and, less pronounced, also along the $4d$ and $5d$ series.[5] The disagreement between experimental and theoretical cohesive energy along the $3d$ series attains its highest value around the middle of the series that is for Mn. Actually, the dip in the cohesive energy observed both experimentally and theoretically for a number of outer electrons around Mn can be attributed to the electronic structure of both the atom and solid, which can favor high-magnetic-moment states. Therefore, the disagreement between theory and experiment about the cohesive energy of Mn can probably be due to an enhancement of the error in the calculation of the electron distributions. On the other hand, the comparison between experimental and theoretical data on the electronic structure of Mn turns out to be difficult, since the pure element has, at room temperature, such a complicated structure both crystallographically and magnetically that an adequate accuracy in an experimental study is a too high demand. Consequently, in order to collect useful experimental data on the electron distribution in Mn, one has to focus on Mn-based alloys having a simple structure. In such a way, high-accuracy data can be collected, the system still maintaining the most important features of the electron distribution of Mn.

fcc Mn alloys can be obtained by adding a suitable amount of Fe and, in this particular case, the electronic structure has been studied experimentally at an adequate accuracy level.[6,7] Another example of Mn in the fcc environment is provided by the intermetallic compounds having the formula MnX_3, where X can be Ni or Pt. These systems have been previously studied[8–10] and, apart from the possible need of a more accurate data treatment of the results, it is found that Mn always has a magnetic moment larger than $3\mu_B$, in agreement with the case of $Mn_{66}Fe_{34}$ (Ref. 7), where the magnetic moment is almost $4\mu_B$. The study of the above-mentioned systems is also interesting because the lattice parameter changes from 3.59 Å in the case of $MnNi_3$ to 3.90 Å in the case of $MnPt_3$, thus allowing for identifying effects possibly related to the atomic volume. Actually, several theoretical investigations[11] have elucidated the relevance of this parameter in establishing electronic structure and magnetic properties of a given element. Finally, we note that, in the case of $MnNi_3$, the magnetic state of the alloy can be changed by varying the state of order,[12] thus identifying the effect of the local environment.

With the aim of getting some information on the electron distribution in Mn with regard to magnetic properties in the fcc environment, we performed a measurement

of spin density of $MnNi_3$ at a low degree of order, and, hence, a low magnetic moment, and an analysis of the available experimental data on totally ordered $MnNi_3$ (Ref. 8) and $MnPt_3$.[9,10] The choice of reanalyzing the already published data[8-10] was dictated by the need of having data which, as referred to different states of the various systems, were internally comparable. Performing in all cases the same analysis of the experimental data allows for a reasonable identification of stable magnetic structures of Mn when embedded in a fcc environment and for deducing the symmetry of the spin density, which has been proved to play a fundamental role in comparing theory and experiment.[1,2] Moreover, considering that in many cases Mn exhibits a magnetic moment close to $4\mu_B$, i.e., the maximum magnetic moment allowed in Mn, some information on the general electron distribution can be obtained assuming an almost full up-spin band.[1] Such an experimental information can be useful when compared with the electronic structure of fcc Mn, calculated by means of first-principle approaches,[13,14] as well as with studies of stability of the magnetic structure by means of Stoner-like criteria.[15]

II. EXPERIMENT AND DATA REDUCTION

The experiment was performed on the polarized-neutron diffractometer installed at the 1-MW Training, Research and Isotope Production Reactor of the Centro Ricerche Energia, Casaccia (Rome). A standard experimental setup was employed: $Co_{0.92}Fe_{0.08}$ polarizing monochromator, neutron-spin reversal at a frequency of 5 Hz, and 0.7-T magnetic field at the sample. The sample was a slab-shaped crystal having dimensions $1\times1.8\times0.07$ cm^3, with the extended face parallel to the (100) plane. The crystal composition was determined by chemical analysis and by x-ray emission and the actual formula was found to be $MnNi_{3.55}$.

The crystallographic structure of the compound ($L1_2$ type) is based on a cubic fcc cell with two sets of nonequivalent crystallographic sites, namely, corner and face sites. When the stoichiometric system is ideally ordered, corners (A sites) are occupied by Mn and faces (B sites) by Ni. The structure factors fall in two classes, F and L:

$$F:\ F_{hkl}(F)=a_A+3a_B \quad \text{if } h,\ k, \text{ and } l \text{ have the same parity},$$

$$L:\ F_{hkl}(L)=a_A-a_B \quad \text{otherwise},$$

where a_l is the total scattering amplitude of the lth site. F refers to the fundamental reflections while L indicates the superlattice ones. The state of order of the sample is determined by the long-range order parameter S, which we define as

$$S=\frac{F(L)}{(a_{\mathrm{Mn}}-a_{\mathrm{Ni}})},$$

where $F(L)$ is the *measured* structure factor of the superlattice reflections. Since we were interested in a relatively low degree of order, an appropriate thermal treatment was applied to the sample. We started from the complete disordered state by heating the crystal up to 700 °C for 1h under vacuum (10^{-6} Torr), then we annealed the sample for 207 h at 420 °C, that is just below the order-disorder transition temperature. Finally, the sample was cooled down to room temperature in about half an hour. The resulting degree of order of the sample was determined by measuring the intensity ratios of superlattice to fundamental reflections, thus avoiding the absolute measurement of the superlattice intensity. In order to make negligible the effect of half-wavelength contamination in measuring the superlattice intensity, a Ge(111) monochromator was employed. The integrated intensities of (100), (200), (300), and (400) reflections were measured at two different wavelengths (1.421 and 1.104 Å) in order to deduce the intensity ratios as well as the extinction free-structure factors. From these measurements we got $S=0.259\pm0.002$. Using the measured value of S and the chemical composition of the sample, it was possible to deduce the occupation probability of the two sites by the two atoms. We have

$$p_{\mathrm{Mn}}(\mathrm{Mn})=\tfrac{3}{4}S+x,$$

$$p_{\mathrm{Mn}}(\mathrm{Ni})=1-p_{\mathrm{Mn}}(\mathrm{Mn}),$$

$$p_{\mathrm{Ni}}(\mathrm{Mn})=1-p_{\mathrm{Ni}}(\mathrm{Ni}),$$

$$p_{\mathrm{Ni}}(\mathrm{Ni})=1+\frac{p_{\mathrm{Mn}}(\mathrm{Mn})-4x}{3},$$

where $p_l(X)$ is the probability of finding an atom X at the site l and x is the Mn concentration.

The flipping ratios of 22 reflections, including 15 fundamental reflections and 7 superlattice reflections, were measured at room temperature using an incoming-neutron wavelength $\lambda=0.89$ Å. Standard corrections for incomplete polarization of the incoming beam, flipping efficiency, and half-wavelength contamination were applied. Although the extinction effect was found to be very small, we applied a simple kinematical approximation to correct the measured flipping ratios:

$$I_\sigma=I_0[1-\exp(-\Sigma_\sigma t)],$$

$$\Sigma_\sigma=\alpha|F_N|^2\frac{1+\gamma^2+2p_\sigma\gamma}{\sin(2\theta)},$$

where I_σ and I_0 are diffracted and incoming intensities, respectively, t is the neutron path inside the sample, σ is the index of the neutron spin, 2θ is the scattering angle, F_N is the nuclear structure factor, γ is the ratio of magnetic to nuclear structure factor, p_σ is the incoming-neutron polarization, and α is a parameter to be fitted to the experimental data. This approximation turned out to work fairly well in the present case, though the amount of extinction was almost negligible ($\alpha=0.02$). By applying such a correction we deduced the values of the flipping ratios of all reflections. The bulk magnetization of the present system was measured on the same sample employed in the neutron-scattering experiment using a ballistic magnetometer.

The neutron-diffraction data thus obtained were put on an absolute scale assuming $b_{\mathrm{Mn}}=-3.73$ fm and

TABLE I. Experimental structure factors of the present sample at a low degree of order.

h	k	l	$\sin\theta/\lambda$ (Å^{-1})	F_G (μ_B/unit cell)
0	0	0	0	1.152±0.012
1	1	1	0.2416	0.720±0.013
2	0	0	0.2789	0.620±0.013
2	2	0	0.3945	0.391±0.011
3	1	1	0.4626	0.267±0.013
2	2	2	0.4831	0.254±0.014
4	0	0	0.5579	0.130±0.016
3	3	1	0.6079	0.155±0.021
4	2	0	0.6237	0.100±0.014
4	2	2	0.6833	0.086±0.024
5	1	1	0.7247	0.003±0.032
3	3	3	0.7247	0.055±0.021
4	4	0	0.7890	0.035±0.017
5	3	1	0.8251	0.006±0.024
6	0	0	0.8368	−0.003±0.025
4	4	2	0.8368	0.086±0.018
1	0	0	0.1395	0.343±0.011
1	1	0	0.1972	0.301±0.011
2	1	0	0.3119	0.163±0.011
2	1	1	0.3416	0.139±0.011
3	0	0	0.4184	0.073±0.011
2	2	1	0.4184	0.080±0.011
3	1	0	0.4410	0.092±0.011

$b_{Ni}=10.3$ fm and using the experimentally determined value of the degree of order. The corrected structure factors are reported in Table I, where the quoted errors take into account both the statistical errors and the uncertainties affecting the applied corrections.

III. DISCUSSION AND COMPARISON TO OTHER MnX_3 SYSTEMS

The structure factor data presented in the previous section can be used to derive some information on the possible magnetic states of Mn in a fcc environment. As a consequence of the low degree of order of the present alloy, an appreciable amount of Mn atoms is found at both sites in the unit cell. Therefore, all Mn atoms have an appreciable average number of other Mn atoms as first-nearest neighbors. It has been already observed[7] that a large number of Mn first-nearest neighbors induces an antiferromagnetic alignment of Mn with respect to the total magnetic moment of the system. In such a situation it is clear that, if no hypothesis about the magnetic moments of the various atoms is done, there is no way of obtaining some quantitative information about the magnetic state of the various atoms. Moreover, it is evident that the analysis of a single system is of little help in view of the complexity of the present magnetic structure.

To derive meaningful data from the present results we have performed the same analysis successfully employed in other systems.[1,2] Using the structure factors F_G given in Table I, the magnetic moments within the Wigner-Seitz (WS) cells centered around each site can be deduced by the following relationship:

$$\mu_l=\frac{1}{\Omega_0}\sum_{\mathbf{G}} F_G \int_{\mathrm{WS}(l)} \exp(i\mathbf{G}\cdot\mathbf{r})d\mathbf{r}\ , \tag{1}$$

where $\mathbf{G}$ is a reciprocal-lattice vector, Ω_0 is the unit-cell volume, and the integral is over the Wigner-Seitz cell WS(l) centered around the lth site. As already observed,[1] the fundamental reflections, with the exception of (000), do not contribute to the site magnetic moments given by the integral in Eq. (1), so that the extinction correction does not introduce an appreciable error on the μ_l's. Considering that only the superlattice reflections contribute to the value of the magnetic moments, the knowledge of the long-range order parameter S is extremely important, as the structure factors of the superlattice reflections are proportional to S. The site magnetic moments calculated according to Eq. (1) are reported in Table II together with those of Refs. 8–10, obtained applying the same procedure.

The simplest hypothesis which can be done in order to interpret the results of Table II consists in assuming average magnetic moments of the two atoms independent of the site in each system. With this assumption, the magnetic moments of the two atoms turn out to be $\mu(\mathrm{Mn})=1.597\mu_B$ and $\mu(\mathrm{Ni})=-0.102\mu_B$ in $MnNi_{3.55}$, $\mu(\mathrm{Mn})=3.369\mu_B$ and $\mu(\mathrm{Ni})=0.217\mu_B$ in $MnNi_3$, which is assumed perfectly ordered,[8] $\mu(\mathrm{Mn})=3.786\mu_B$ and $\mu(\mathrm{Pt})=0.092\mu_B$ in $MnPt_3$,[9] $\mu(\mathrm{Mn})=3.754\mu_B$ and $\mu(\mathrm{Pt})=-0.163\mu_B$ in $MnPt_{2.57}$.[10] The results thus obtained for the present sample are clearly very unlikely, while in the case of $MnNi_3$ the magnetic moment of Mn is smaller than those found in $MnPt_3$, $MnPt_{2.57}$, and in Ref. 7 and also the value for Ni is depressed with respect

TABLE II. Site occupancy probabilities (see text) and site magnetic moments for the present sample and those of Refs. 8–10.

	P_{Mn}(Mn)	p_{Ni}(Ni)	p_{Pt}(Pt)	μ_{Mn}/μ_B	μ_{Ni}/μ_B	μ_{Pt}/μ_B
Present data	0.423±0.010	0.836±0.010		0.617±0.012	0.177±0.005	
Ref. 8	1	1		3.369±0.030	0.217±0.003	
Ref. 9	0.928±0.01		0.978±0.01	3.521±0.050		0.173±0.005
Ref. 10	$1^{+0}_{-0.01}$		0.956±0.01	3.754±0.030		0.009±0.005

to that currently reported in literature for several systems. In view of the too low magnetic moments of both atoms in $MnNi_3$, which could be a consequence of a nonunitary long-range-order parameter, these data will be discarded in performing a more quantitative analysis. The negative value of μ(Pt) in $MnPt_{2.57}$ can be interpreted as a direct evidence of an antiferromagnetic alignment of Mn.

To get meaningful magnetic moments for the system $MnNi_{3.55}$, further information about the electronic structure of both Mn and Ni is necessary. Because of the intrinsic partial disorder affecting the present sample, a calculation of the electron distribution in perfectly ordered $MnNi_3$ compound is of little help in interpreting our experimental data. Moreover, since some guess is necessary in order to gain more information from the experimental data, we preferred to resort to a simple phenomenological model of the electronic structure of Mn and Ni. Therefore, we performed a density-of-states calculation for both Mn and Ni in the fcc paramagnetic phase at a lattice parameter $a_0=3.585$ Å, i.e., the value for the present sample. To investigate the possible magnetic phases of Mn and Ni, we have applied a rigid-band splitting to the calculated paramagnetic density of states. Calculations have been done using the Slater and Koster approximation as described by Papacostantopoulous[16] and using the parameters derived therein. The number of electrons having spin σ and occupying the states corresponding to the irreducible representations Γ_1, Γ_{15}, Γ_{12}, and $\Gamma_{25'}$ can be written as

$$n_{\sigma\nu}=\int_{-\infty}^{\varepsilon_F}\rho_\nu(\varepsilon-U_\nu n_{-\sigma})d\varepsilon\ , \tag{2}$$

where ν indicates the irreducible representation

$$n_\sigma=\sum_\nu n_{\sigma\nu}$$

and U_ν is a splitting parameter which is zero for Γ_1 and Γ_{15} and has a fixed value U for Γ_{12} and $\Gamma_{25'}$. $\rho_\nu(\varepsilon)$ is the density of states of the paramagnetic phase. The Fermi energy ε_F is determined by fixing the total number of electrons. When Eq. (2) is satisfied for a given set of occupation numbers $n_{\sigma\nu}$, the magnetic moment as well as the contributions to the magnetic moment from the projection of the magnetic moment density into the irreducible representations can be deduced. On the other hand, the latter quantities can be obtained experimentally by analyzing the aspherical contributions to the neutron and x-ray structure factors. Mathematically, Eq. (2) admits at least one solution for all nonzero U's, but the physical meaning of the solution is related to the stability of a given magnetic phase. To this purpose we observe that Eq. (2) can be written as follows:

$$\begin{aligned} n_{\sigma\nu}&=\int_{-\infty}^{\varepsilon_F}\rho_\nu(\varepsilon-U\bar{n}_{-\sigma})d\varepsilon\ ,\\ n_\sigma&=\bar{n}_\sigma\ . \end{aligned} \tag{3}$$

In such a way, Eq. (2) is regarded as a system of two equations plus the condition for determining ε_F. For a fixed value of the parameter U, the different solutions of Eq. (3) can be considered stable or unstable depending on the derivative of n_σ with respect to $\bar{n}_\sigma$. The stability of a solution $n_\sigma=\bar{n}_\sigma$ is guaranteed if

$$|\delta n_\sigma|<|\delta\bar{n}_\sigma| \quad \text{or equivalently} \quad \frac{|dn_\sigma|}{|d\bar{n}_\sigma|}<1\ , \tag{4}$$

that is, when a fluctuation of $\bar{n}_\sigma$ induces a smaller fluctuation on n_σ. When such a condition is satisfied, Eq. (3) can be solved iteratively since in the region where Eq. (4) holds n_σ, as a function of $\bar{n}_\sigma$, verifies the Lipshitz condition. Using Eq. (4) under the condition that the total number of electrons is constant, we get

$$P(U)=\frac{\{[\rho_\uparrow(\varepsilon_F)]^2+[\rho_\downarrow(\varepsilon_F)]^2\}U}{\rho_\uparrow(\varepsilon_F)+\rho_\downarrow(\varepsilon_F)}<1\ . \tag{5}$$

Equation (5) is a generalization of the well-known Stoner criterion as it holds for all magnetic moments which are solutions of Eq. (2). As a consequence, the paramagnetic phase is stable if

$$\rho(\varepsilon_F)U<1\ , \tag{6}$$

where $\rho(\varepsilon_F)=\rho_\uparrow(\varepsilon_F)=\rho_\downarrow(\varepsilon_F)$ is the density of states per spin at the Fermi level. Equation (6) is the more common form of the Stoner criterion. The magnetic moments of Mn and Ni obtained from the calculations outlined above are shown in Figs. 1(a) and 1(b) where the Stoner parameter $P(U)$ is also plotted as a function of U. As we can see from Fig. 1(a), the present approach suggests that Mn has only one stable magnetic phase which corresponds essentially to the maximum magnetic moment attainable in this system, namely, about $3.8\mu_B$. This high-magnetic-moment phase is fairly stable as a consequence of the low Stoner parameter calculated by Eq. (5). The results reported in Fig. 1(b) show that, in the case of Ni, there is still a stable phase with a magnetic moment of about $0.6\mu_B$, but it is confined in an extremely small range of U. Finally, in Fig. 1(c) we report the magnetic moments corresponding to the representation Γ_{12} as a percentage (p_m) of the total magnetic moment. For both Mn and Ni, p_m is essentially constant over the whole range of U.

According to these results and those reported in Table II, we note that the analysis of all the data cannot be carried out assuming that Ni and Mn have a magnetic moment independent of composition and state of order as such an hypothesis is not compatible with the data of Table II. Therefore, in order to explain the strong change of the total as well as of the site magnetic moments with the state of order in these systems, we can *assume* that the magnetic moment of Mn atoms is always the same, but allowing for a change of sign of this magnetic moment as a consequence of the local environment. This assumption was originally proposed by Weiss discussing the magnetic state of fcc iron.[17,18] Having made a hypothesis for the atomic magnetic moments, we can only check its compatability with available data since the number of variables in the present system is too large to determine univocally the electronic structure of the various atoms. If the absolute values of the magnetic moments of Mn and Ni are μ(Mn) and μ(Ni), the magnetic moment at the site l of the alloy is given by

$$\mu_l = p_l(\mathrm{Mn})[1-2x_l^-]\mu(\mathrm{Mn}) + [1-p_l(\mathrm{Mn})]\mu(\mathrm{Ni}) , \quad (7)$$

where $p_l(X)$ is the already defined probability that the site l is occupied by the atom X and x_l^- is the probability that the Mn atom at the site l has a negative magnetic moment. In order to proceed further, we have to make some assumptions on μ(Mn) and μ(Ni). We can observe that, in the case of $Fe_{66}Mn_{34}$,[7] the magnetic moment of Mn resulted to be $3.90\mu_B$, while in $MnPt_3$ (Ref. 9) and $MnPt_{2.57}$ (Ref. 10) the Mn magnetic moment was $3.75\mu_B$. A similar high magnetic moment is also observed in diluite Ni-Mn (Ref. 19) as well as in Pd-Mn (Ref. 20) alloys. All these values are in reasonable agreement with the theoretical estimates of Fig. 1. Therefore, we assumed $\mu(\mathrm{Mn})=3.7\mu_B$ and $\mu(\mathrm{Ni})=0.6\mu_B$. In the case of Ni, the chosen value of μ(Ni) is a reasonable one in agreement with several experimental data and with the estimates of Fig. 1(b). Then, using Eq. (7), x_l^- at Mn and Ni sites can be derived. We got $x_{\mathrm{Mn}}^- = 0.413 \pm 0.005$ and $x_{\mathrm{Ni}}^- = 0.767 \pm 0.005$. These estimates can be compared with those derived under the assumptions of no short-range order and a negative magnetic moment for the Mn atom when the number of Mn first-nearest neighbors is greater than a given number n_0. In this condition, as the number of Mn first-nearest neighbors follows a Poisson's distribution, we have

$$x^- = \sum_{r=n_0+1}^{\infty} \exp[-n]\frac{n^r}{r!} , \quad (8)$$

where n is the average number of Mn atoms first-nearest neighbors. Equation (8) gives a reasonable description of the distribution of the negative-magnetic-moment states of Mn. In Fig. 2 we report x^- as deduced from Eq. (8), assuming $n_0=1$, 2, and 3 in comparison with the experimental values obtained at the two crystallographic sites in the present sample. The point $x^-=1$ at $n=4$, deduced from the results of Refs. 9 and 10, has been added in Fig. 2. As we can see, the present population of negative-magnetic-moment states is reasonably well described by the random model of Eq. (8) if $n_0=1$, thus indicating the relevance of the local environment in determining the ferromagnetic or antiferromagnetic alignment of Mn.

From the above analysis we can conclude that a reasonable model of the Mn atoms in these systems pro-

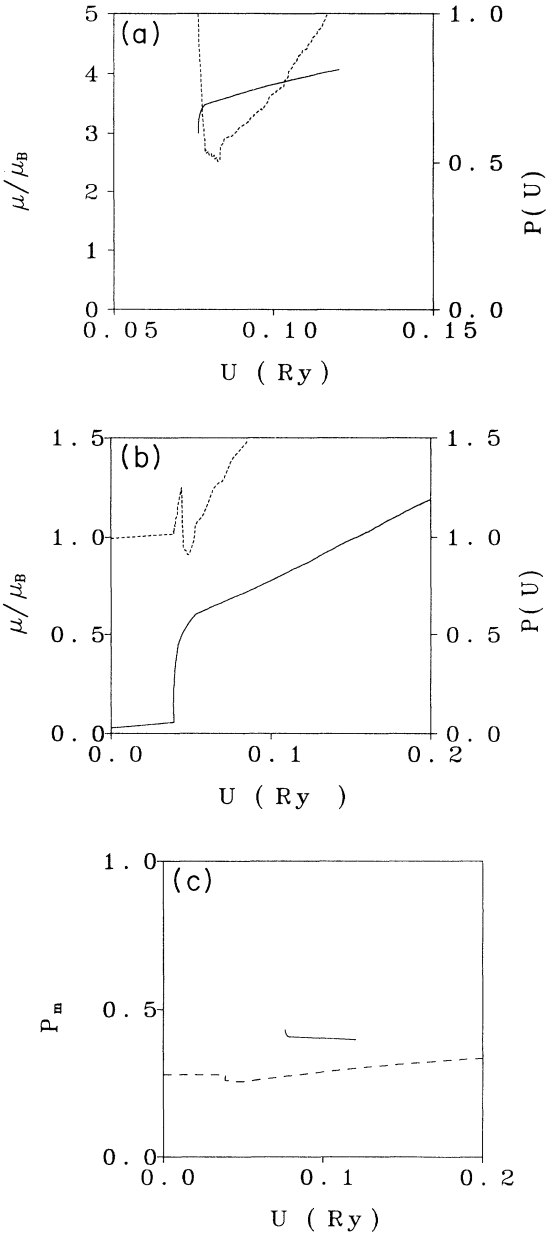

FIG. 1. (a) Total magnetic moment (solid line) and Stoner parameter $P(U)$ (dashed line) vs U calculated applying the present theoretical model for Mn. (b) Total magnetic moment (solid line) and Stoner parameter $P(U)$ (dashed line) vs U calculated applying the present theoretical model for Ni. (c) Percentage p_m of Γ_{12} symmetry magnetic moment calculated by applying the present theoretical model for Mn (solid line) and Ni (dashed line).

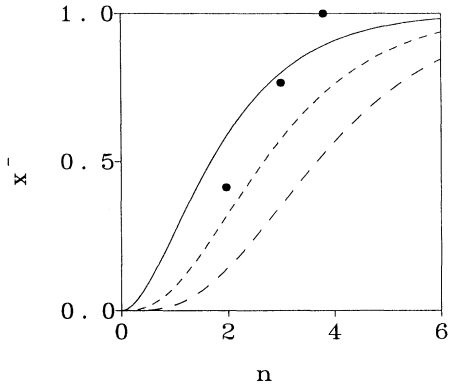

FIG. 2. Probability of the negative-magnetic-moment state of Mn as a function of the average number of Mn atoms first-nearest neighbors. Dots: experimental results obtained from the present analysis (see text). Lines: random model described in the text. Solid line $n_0=1$, short-dashed line $n_0=2$, dashed line $n_0=3$.

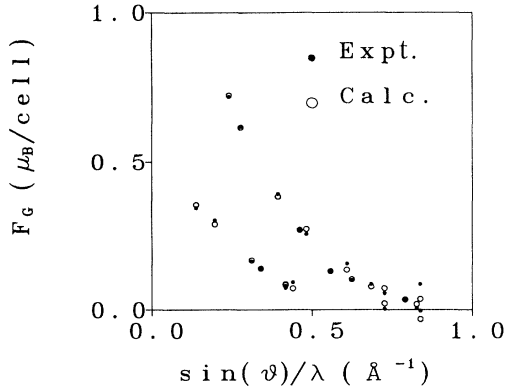

FIG. 3. Fit of the present experimental magnetic structure factors to Eq. (9). The upper points refer to fundamental reflections, while the lower ones refer to the superlattice reflections.

vides for a high-magnetic-moment state of Mn but with fluctuating sign. Such a model accounts for the data available around the stoichiometric composition. This picture is directly related to the spin-glass behavior observed in disordered samples at low temperature.[21] Moreover, even close to the present composition, where the spin-glass behavior appears to be absent, an anomalous trend of the bulk magnetization versus temperature[12] is found, thus suggesting that the concentration of Mn atoms with negative magnetic moments is a function of temperature.

To get further insight into the electronic structure of both Mn and Ni in the present system, we also analyzed the symmetry of the spin density of each site. In general, we can write[1,2]

$$F_G=\sum_l \cos(\mathbf{G}\cdot\mathbf{R}_l)[\mu_l f_l(G)+\mu_l^{\text{asph}} f_l^{\text{asph}}(\mathbf{G})] , \quad (9)$$

where $\mathbf{R}_l$ is the position of the lth site in the unit cell, μ_l is the site magnetic moment given in Eq. (1), $f_l(G)$ is the spherical site form factor, μ_l^{asph} is an aspherical magnetic moment, and $f_l^{\text{asph}}(\mathbf{G})$ is the corresponding aspherical form factor. Taking into account the four irreducible representations Γ_1, Γ_{15}, Γ_{12}, and $\Gamma_{25'}$, the aspherical form factor can be written as

$$f_l^{\text{asph}}(\mathbf{G})=A(\hat{\mathbf{G}})f_l^{(4)}(G) , \quad (10)$$

where $A(\hat{\mathbf{G}})$ is the appropriate angular factor[22] and $f_l^{(4)}(G)$ is directly related to the actual spin density.[2] $f_l(G)$ and $f_l^{(4)}(G)$ can be deduced by applying the same procedure leading to Eq. (1). The following equations are easily obtained:

$$f_l(Q)=\frac{1}{\Omega_0\mu_l}\sum_G F_G\int_{\text{WS}(l)} j_0(Qr)\exp[i\mathbf{G}\cdot\mathbf{r}]d\mathbf{r} ,$$
$$f_l^4(Q)=\frac{1}{\Omega_0\mu_l}\sum_G F_G\int_{\text{WS}(l)} j_4(Qr)\exp[i\mathbf{G}\cdot\mathbf{r}]d\mathbf{r} , \quad (11)$$

where $j_n(x)$ is the spherical Bessel function of nth order. Equations (9)–(11) were used to fit the present data as well as those of Ref. 8. The aspherical magnetic moments so derived are reported in the first two columns of Table III, while the structure factors calculated for the present sample with the help of Eq. (9) are shown in Fig. 3 in comparison with the experimental data. The agreement between the fit and the measured structure factors is quite good ($\chi^2=21$). First of all, we observe that, in the present sample, the aspherical magnetic moment at the Ni site is of the same order of magnitude as the total magnetic moment at this site (reported in Table II), evidently an absurd situation. Consequently, the Ni magnetic moment is expected to be larger than the site mag-

TABLE III. Aspherical contributions to site (first two columns) and atomic (second two columns) magnetic moments for the present sample and that of Ref. 8. Theoretical and experimental percentages p_m of Γ_{12} symmetry magnetic moment (see text) are reported for Mn and Ni in the last two columns.

	$\mu_{\text{Mn}}^{\text{asph}}/\mu_B$	$\mu_{\text{Ni}}^{\text{asph}}/\mu_B$	$\mu(\text{Mn})^{\text{asph}}/\mu_B$	$\mu(\text{Ni})^{\text{asph}}/\mu_B$	p_m (model)	p_m (expt.)
Present data	−0.083±0.020	−0.145±0.040	0.13±0.04	−0.17±0.04		
Ref. 8	0.28±0.10	0.01±0.10	0.28±0.10	0.01±0.10		
Ni					0.15	0.303±0.025
Mn					0.403	0.416±0.004

TABLE IV. Occupation numbers of the various electronic states in fcc Mn as deduced from the present analysis of the experimental data (see text) and from the present theoretical model.

	$n_{\Gamma_{12}\uparrow}$	$n_{\Gamma_{25'}\uparrow}$	$n_{\Gamma_{12}\downarrow}$	$n_{\Gamma_{25'}\downarrow}$	$n_{\Gamma_1}+n_{\Gamma_{15}}$
Expt.	2	3	0.47	0.83	0.35
Model	1.99	2.94	0.50	0.73	0.42

netic moment, thus supporting again the idea of a large number of Mn atoms present with a negative magnetic moment at the Ni site. To obtain the aspherical magnetic moment of the various *atoms*, Eq. (7) can also be applied to the case of the aspherical contribution using x_l^- previously derived and the μ_l^{asph}'s. Results thus obtained are reported in the second two columns of Table III. The comparison between the present system and that of Ref. 8 shows that, within the experimental errors, the aspherical magnetic moments for both Mn and Ni can be considered the same. In the last two columns of Table III, the Γ_{12} percentages of the total magnetic moments (p_m) of Ni and Mn are reported in comparison with the values deduced in the present model. For Mn the Γ_{12} symmetry state results to be more populated, while in the case of Ni the $\Gamma_{25'}$ symmetry state is favored, as for the pure metal.[22]

Finally, we remark that, from the present data, the magnetic state of Mn within the fcc environment corresponds to a high-magnetic-moment phase with the up-spin $3d$ band almost full. Therefore, it is possible to derive the occupations of the various electronic states with the farther simple assumption that the up- and down-spin occupations of the Γ_1 and Γ_{15} states are the same. The resulting data are reported in Table IV together with those deduced from the present calculation.

As a last statement we can say that the collection of experimental data, together with the phenomenological model presented here, give a substantial ground to the idea that positive- and negative-magnetic-moment states of Mn coexist in the MnX_3 systems when not fully ordered. The data derived from the model, which is based on the LDA calculation of the electron distribution in the paramagnetic phase, account correctly for the magnetic moments we inferred from all the experimental data, even though, as it has been already observed in other systems, the electron distribution in the various symmetry states is not correctly reproduced. In view of the great importance of Mn, the present system as well as the other companion systems should be analyzed in greater detail in order to determine the electron distribution and the possibly present fluctuations of the magnetic state.

ACKNOWLEDGMENT

The authors wish to thank G. Mazzone for many critical comments and helpful discussions.

[1]E. Di Fabrizio, G. Mazzone, C. Petrillo, and F. Sacchetti, Phys. Rev. B **40**, 9502 (1989).
[2]L. Dobrzynski, C. Petrillo, and F. Sacchetti, Phys. Rev. B **42**, 1142 (1990).
[3]*Theory of the Inhomogeneous Electron Gas,* edited by S. Lundqvist and N. H. March (Plenum, New York, 1983).
[4]C. S. Wang and B. M. Klein, Phys. Rev. B **24**, 3393 (1981).
[5]V. L. Moruzzi, J. F. Janak, and H. R. Williams, *Calculated Electronic Properties of Metals* (Pergamon, New York, 1978).
[6]C. Andreani, G. Mazzone, and F. Sacchetti, J. Phys. F **17**, 1419 (1987).
[7]P. Bisanti, G. Mazzone, and F. Sacchetti, J. Phys. F **17**, 1425 (1987).
[8]A. Delapalme, Solid State Commun. **5**, 769 (1967).
[9]B. Antonini, F. Lucari, F. Menzinger, and A. Paoletti, Phys. Rev. **187**, 611 (1969).
[10]F. Menzinger, F. Sacchetti, and M. Romanazzo, Phys. Rev. B **5**, 3778 (1972).
[11]V. L. Moruzzi and P. M. Marcus, Phys. Rev. B **38**, 1613 (1988), and references cited therein.
[12]A. Paoletti, F. P. Ricci, and L. Passari, J. Appl. Phys. **37**, 3236 (1966).
[13]V. L. Moruzzi, P. M. Marcus, and J. Kubler, Phys. Rev. B **39**, 6957 (1989).
[14]G. Fuster, N. E. Brener, J. Callaway, J. L. Fry, Y. Z. Zhao, and D. A. Papacostantopoulos, Phys. Rev. B **38**, 423 (1988).
[15]G. L. Krasko, Phys. Rev. B **36**, 8565 (1987).
[16]D. A. Papacostantopoulos, *Handbook of the Band Structure of Elemental Solids* (Plenum, New York, 1986).
[17]R. J. Weiss, Proc. Phys. Soc. London **82**, 281 (1963).
[18]F. Duprè, F. Menzinger, and F. Sacchetti, J. Phys. F **11**, 2179 (1981).
[19]J. W. Cable and H. R. Child, Phys. Rev. B **10**, 4607 (1974).
[20]R. E. Parra, A. C. Gonzales, and R. A. Lopez, J. Phys.: Condens. Matter **2**, 7309 (1990).
[21]J. W. Cable, R. M. Nickow, and Y. Tsunoda, Phys. Rev. B **36**, 5311 (1987).
[22]F. Menzinger and F. Sacchetti, Nukleonika **24**, 737 (1979).